Appl Phys B (2009) 94: 127–132
DOI 10.1007/s00340-008-3295-9

Applied Physics B
Lasers and Optics

Laser desorption studies using laser-induced fluorescence of large aromatic molecules

G.P. Smith · B. Krancevic · D.L. Huestis · H. Oser

Received: 24 June 2008 / Revised version: 5 September 2008 / Published online: 15 November 2008

Abstract Pulsed laser desorption of non-volatile organic dye molecules paraterphenyl and tetra-t-butyl-p-quinquephenyl (QUI) was studied using gas phase ultraviolet laser induced fluorescence, following heating of a steel substrate by a pulsed 1.06-μm Nd:YAG laser. The fluorescence signal intensity is linear in concentration up to at least 30 monolayers and shows infrared power threshold behavior, as expected for evaporation, at ∼0.2 J/cm^2. Similar signal levels were also observed in air, with 532-nm heating, and using other metallic or dark black surfaces.

PACS 68.43.Vx · 79.20.Ds · 44.35.+c

1 Introduction

Detection and analysis of large molecules by many mass spectrometric and laser spectroscopic methods requires sample preparation technologies to ultimately deliver these non-volatile species into the gas phase. This is particularly apparent for the problem of remote standoff detection of explosive devices. Residues of nitro compounds are likely present on surfaces, but have very low vapor pressures. A sensitive laser method is available to detect these substances, based on a sequential three-ultraviolet-photon process in the gas phase: photodissociation of the R-NO_2 compound, photodissociation of the NO_2 product, and laser-induced fluorescence (LIF) detection of the vibrationally excited NO that is produced [1–3]. This method requires first irradiating or heating the sample to release the surface-absorbed nitro compounds. Therefore, one must consider what laser wavelength and power are best suited to this purpose from a distance, and how any laser desorption process would vary with surface properties. The ambient vapor pressure of the common explosive molecule RDX (cyclotrimethylenetrinitramine) is only 10^{-8} torr [4], but a monolayer if vaporized can generate concentrations of $3 \times 10^{14}/\text{cm}^3$. This is a readily detectable amount of vapor [3], and a reasonable amount of residue to expect [5]. The volatilization process needs to be designed to effectively deliver such yields under various conditions, without resulting in premature (ablative) formation of non-photolytic NO decomposition products. Therefore, we have conducted some preliminary experiments to examine laser evaporation rates, mainly with respect to laser power and surface coverage. We also investigated variations with laser wavelength, pressure, surface material, and adsorbate. This initial work substitutes large organic molecules that fluoresce directly for actual organonitro compounds, in order to avoid the complexity of the NO LIF detection scheme and to focus on the laser desorption process. For most of the experiments, we use 1.06-μm pulsed Nd:YAG laser radiation to heat a stainless steel surface coated with paraterphenyl, $C_{18}H_{14}$, an organic laser dye containing three connected benzene rings. This compound absorbs 266-nm frequency-quadrupled Nd:YAG radiation from another laser, and then fluoresces at 320–370 nm. We performed some runs under ambient conditions, but concentrated on low-pressure experiments to avoid

G.P. Smith (✉) · B. Krancevic · D.L. Huestis · H. Oser
Molecular Physics Laboratory, SRI International, Menlo Park, CA 94025, USA
e-mail: gregory.smith@sri.com
Fax: +1-650-8593196

Present address:
B. Krancevic
Physics Department, Cleveland State University, Cleveland, OH 44115, USA

gas interaction effects and to focus on the laser evaporation process.

There are some previous investigations in the literature of laser desorption, as one might expect, ranging from basic physical studies of simple molecules on clean surfaces [6–8], detailed theories of underlying processes [7, 9–11], desorption of organic molecules [12–14], and use of laser preparation to detect explosive molecules [10, 15–18]. These provide a useful context for our parameterized study. Theoretical interpretations and models of results for metallic (conducting) substrates describe the process as absorption of most of the pulsed laser light in the uppermost few layers, induced by the effect of the intense laser electric field on the electrons. During and after the heating, competing processes of heat loss by conduction into the bulk solid, heat transfer to the adsorbate, and its evaporation kinetics occur. When many monolayers of material are deposited on the surface, one must also consider the possible formation of a near-surface gas bubble that will propel material outward. This theory of competing physical processes suggests that the predominant controlling parameters are laser power, laser pulse length and shape, substrate thermal conductivity, adsorbate vaporization enthalpy (and kinetic preexponential factor), and depth of coverage. The theory can also consider the effect of distributing the laser absorption through a thicker layer of the substrate. Such a scenario might approximate the behavior of a non-conducting material that is still strongly absorbing at the laser wavelength.

Past studies of laser desorption of large molecules tend toward parameterizations of the specific analysis method being developed. There are reports of direct vaporization of polycyclic aromatics by 355-nm ultraviolet (UV) pulsed laser light [13] or by 3.3-μm pulsed infrared (IR) radiation resonant with CH absorptions [12]. Sometimes the same UV or IR laser is used for both desorption and ionization, as in a study of solvated organics on etched silicon surfaces [14]. Some work has also been performed on nitro compounds and actual explosives. Desorption at Nd:YAG 266-nm and 532-nm wavelengths was used to vaporize samples for ionization in mass spectrometric detection development efforts [15, 18]. Other studies applied high-power 248-nm excimer lasers or near-IR lasers to accomplish both desorption and fragmentation of explosives, prior to NO detection by either resonant multiphoton ionization (REMPI) or IR absorption [16, 17]. One brief experimental and modeling study did examine vaporization of RDX on silica using pulsed Nd:YAG (1.06 μm) and CO_2 (10.6 μm) lasers and mass spectrometer (MS) sampling, with mixed results [10]. Our SRI colleagues have recently evaporated RDX off metal substrates in vacuum using 355-nm, 532-nm, and 1064-nm Nd:YAG laser pulses, followed by femtosecond multiphoton ionization and time-of-flight mass spectrometric detection [19].

2 Experimental

Experiments were conducted inside a cell with optical access, continuously evacuated by a mechanical pump to pressures of approximately 30–60 mtorr (measured by a capacitance manometer). A rotating target (1.16 Hz) was heated using lasers pulsed at 10 Hz. A 0.3-cm-diameter 1.06-μm (or 532-nm) Nd:YAG laser beam (∼8-ns duration) irradiated the target at right angles 1 cm off-axis. We can model the exposure of the surface to repeated laser shots with respect to fresh unexposed material in two ways. Assuming that the location on the rotating target exposed on successive laser shots is random, because the sample rotation is not synchronized with the laser, half of the available target area is irradiated in 13.3 s (13 laser shots). This half-life is shown by the arrows in Fig. 3. A second more detailed model uses the approximate geometries and target rotation rate to simulate the exposure pattern. It suggests that, during the first two rotations, i.e. 18 laser shots, new material is exposed each time. For the next rotation of nine shots, about half of the irradiated area has been previously exposed. After that, most of the area is being subject to repeated heating.

The evaporation laser power was varied by adjusting the flashlamp energy on the amplifier stage of the Quanta Ray GCR-4 laser used. Laser power was measured separately using a Molectron EPM-1000 power meter inserted after the last aperture before the cell. Because only the central 3-mm region of the >8-mm-diameter Gaussian laser beam was used, far from its source, the assumption of a fairly uniform spatial distribution should be reasonable. After a 6–50 μs delay, which can be varied up to 240 μs using our external trigger timing circuitry, the Quanta Ray GCR-11 detection laser was fired. The quadrupled (266 nm) or tripled (355 nm) Nd:YAG radiation was filtered by a dichroic mirror and directed parallel to the target roughly 2 mm above the heated spot. Overlap of the two lasers was visually confirmed. The fluorescence signal perpendicular to both laser beams was focused onto a 1P28 photomultiplier tube detector, through interference and long-pass filters (340 ± 20 nm), and processed by boxcar integrator and computer data acquisition systems. The prompt boxcar gate was set 0.1-μs wide, and each computerized data point averaged four laser shots. Figure 1 shows a schematic of the apparatus.

Targets were mounted on the end of a rotating feedthrough driven by a speed-controlled drive motor. The organic dye was applied by spraying the target from a set distance using a drug store cologne atomizer filled with a dilute solution. Solutions were prepared from measured weights and volumes of hexane or methanol solvents. Typical amounts delivered per spray were weighed, and the nominal area coverage was estimated from the spray pattern (roughly 45°) and distance. From this information and the solid density of the organic dye, the mass deposited on the target and

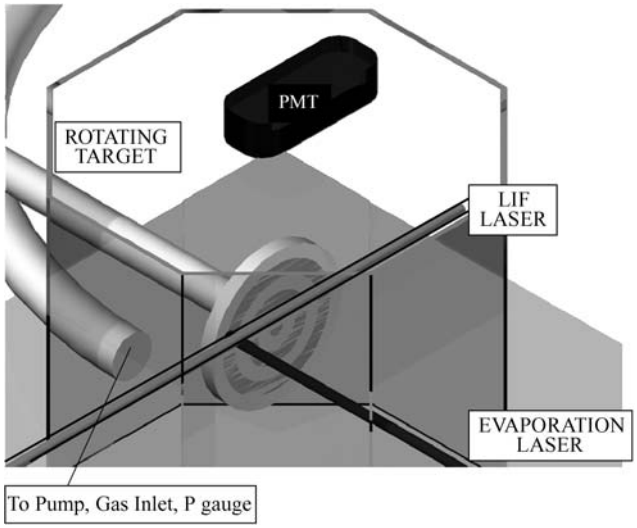

Fig. 1 Schematic of the apparatus chamber for the laser evaporation experiments

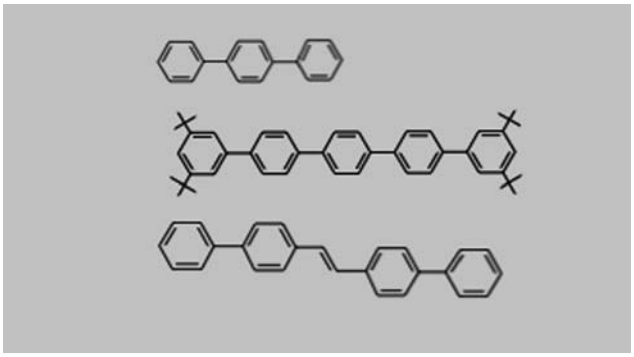

Fig. 2 Chemical structures of the dye molecules used: paraterphenyl, QUI, and diphenylstilbene

the number of monolayers coverage that a uniform layer would represent were determined. In addition to paraterphenyl, $C_6H_5C_6H_4C_6H_5$, experiments were conducted with a heavier dye expected to have even lower vapor pressure and a higher heat of vaporization, QUI, tetra-t-butyl-p-quinquephenyl, $(C_4H_9)_2C_6H_3C_6H_4C_6H_4C_6H_4C_6H_3(C_4H_9)_2$, and also briefly with diphenylstilbene, $C_6H_5C_6H_4CH{=}CHC_6H_4C_6H_5$. Organic structures are given in Fig. 2. These molecules can be excited by the third Nd:YAG laser harmonic at 355 nm, lase in solution near 400 nm, and fluoresce out to the 440-nm detection wavelength chosen. Blank runs with no UV laser or with dye-free solvent coating the target showed no signal. Blocking the IR laser during a run (with pumping) also resulted in fast signal disappearance, which signifies that the evaporate did not linger beyond a few laser repetitions.

We have not independently determined whether a smooth layer of the organic dye results from the evaporative deposition. Examination by an electron microscope did show isolated needle-shaped crystals of paraterphenyl with diameters below 1 μm. This represents a thickness of a few hundred molecules. The fraction of deposited material in this form was not determined. For our experimental and likely analytical situations a non-homogeneous distribution consisting of microcrystals may be more likely. In the presentation of results and discussion, we have parameterized the dye deposition amounts in terms of uniform surface coverage, but it should be kept in mind that this may not properly describe the initial physical situation. To the extent that melting of microcrystals and flow occur rapidly before evaporation, the homogeneous description may still apply. Paraterphenyl melts at 493 K [20].

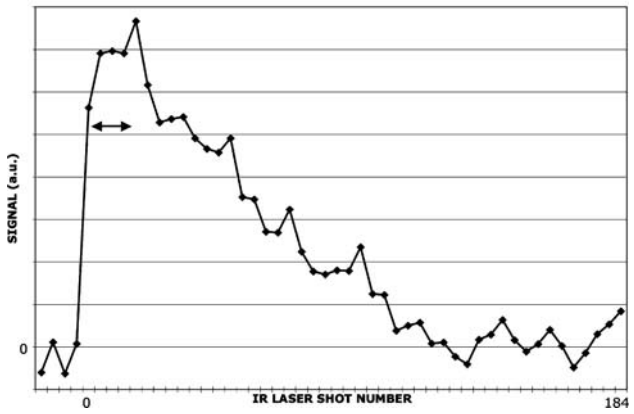

Fig. 3 Laser induced fluorescence signal from paraterphenyl following laser desorption by 1.06-μm radiation. Each *tick and data channel point* is 0.4 s, four laser shots averaged. The *line with arrows* denotes time for half of the available surface area to be exposed to the evaporation laser. Time dependence shows depletion from the steel surface of the rotating target. The LIF probe occurs 10 μs after ∼0.32 J/cm^2 IR irradiation at 1.06 μm, with initial surface coverage of four monolayers

3 Results

Figure 3 shows a typical time trace at low surface coverage (∼four layers) and modest IR laser evaporation power (0.32 J/cm^2). Each point is a sum of four successive laser shots. Higher powers give a sharper initial spike and longer late tail to the signal. As the experiment progresses, more points on the rotating target disk have been irradiated, and an increasing number become exposed a second (or third, etc.) time. The horizontal arrow indicates when half of the rotating target material has been exposed to the laser, according to random exposure of the unsynchronized rotating target. Its rough correspondence with the width of the signal maximum shows that a significant fraction of the heated material is being evaporated upon a single exposure at this power level. The peak is prompt and not wider than the single-exposure 'time'.

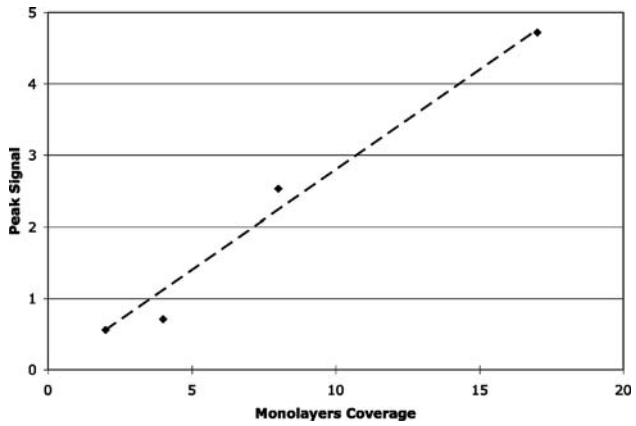

Fig. 4 Dependence of the maximum paraterphenyl laser desorption/laser induced fluorescence signal on the initial surface concentration. IR power ~0.34 J/cm^2

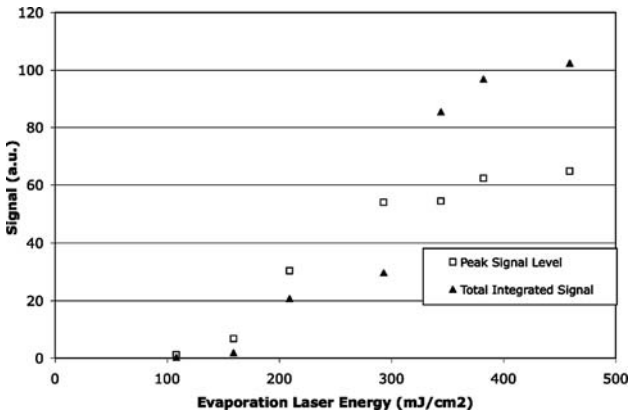

Fig. 5 Dependence of the QUI laser desorption/laser induced fluorescence signal on the infrared laser desorption power. Both initial signal level (*squares*) and integrated total signal (*triangles*) are shown

However, some declining signal does persist for several repeated exposures. (Recall that the models of the experiment indicate that after ~28 shots, i.e. seven data points, most of the surface has been exposed.) Part of this is material unevaporated by its first exposure. This may also represent evaporation from outer regions of the exposed ring, where overlap with the circular laser beam covers a smaller region, the intensity at the laser beam edge may be less, and more rapid diffusive cooling of the surface at the edge of the heated area may happen. One may also interpret the decaying, longer-time signal as partly due to thermally induced diffusion of paraterphenyl from edge areas into target areas recently cleansed by vaporization, whereby a second larger area is also sampled. Some larger microcrystals could also require two or more heating episodes to vaporize completely. In some runs at high laser power, intermittent signal spikes will also appear at even longer exposure times. What is apparent from this behavior is that the total signal from a laser-evaporated sample can be increased by applying repeated laser shots, but any advantage gained by multiple heating rapidly diminishes. Most of the thin sample can be vaporized in a single pulse.

If this mostly complete laser evaporation takes place, and thus if the method is to offer a potential for quantitative sample preparation, linearity of the signal with the amount of deposited organic dye needs to be demonstrated. Figure 4 plots the LIF signal as a function of the amount of paraterphenyl sprayed onto the steel washer surface, with laser heating pulse energies of 0.34 J/cm^2. The behavior plotted is for the maximum signal summed over five channels (20 laser shots, 65% net surface area irradiation). The demonstrated linearity is shown by the dashed line, and also holds for the total integrated signal which includes the later declining portion. Another set of runs indicated that the linear concentration response continues up to an average coverage of 35 monolayers. It may seem that at some point one would expect a change in behavior, at the transition from surface heating and evaporation to heating of bulk paraterphenyl, especially if crystalline material begins to form at higher concentrations and larger sizes. Some theoretical work suggests boiling at the surface below the outer layers of absorbate at high coverages, leading to a violent bursting and droplet formation [11]. These issues need further experimentation, although no sign of such complexities is apparent in the present data.

An important parameter to determine is the evaporation signal response to IR laser power. Sufficient power is desired to evaporate most of the surface molecules, without decomposing the molecules or otherwise ablating surfaces. We performed such a study, for about 17-monolayer nominal coverage, looking at both the peak signal and the summed signal from multiple laser shots. The peak or single-shot signal has a clear power threshold, near 0.16 J/cm^2 for paraterphenyl. Below this point there is little signal and significantly higher power levels do not increase the intensity. One would expect such behavior from evaporative phenomena. The total signal does show some continued increase at higher powers, perhaps from the outward bleeding of the effective area from various causes, as described previously. This increase is associated with the longer-time signal tail. Results are shown for a similar power dependence with the dye QUI in Fig. 5. The same behavior is seen, although the threshold for evaporation is at a higher power level. The laser energies for the data points are approximate values for laser amplifier flashlamp energy settings of 0, 15, 20, 30, 40, 50, and 60 J/pulse. This data was taken at a 10-μs delay and approximately two monolayers (average) of QUI deposited on the steel target. (Uncertainty is difficult to estimate for such parametric studies as Figs. 4 and 5. While we followed a consistent protocol in each series, run-to-run differences in IR and UV laser power and in surface spray coverage of 10% might be expected. This predicts a 20% uncertainty, in line with our experience for repeated experiments.)

Experiments were also conducted for other target substrate materials, typically with 17-monolayer coverage of paraterphenyl and a 50-μs delay. We used 0.34 J/cm^2 IR laser power, and increased it to 0.56 J/cm^2 if no signal appeared. Signals were observed from aluminum, copper, black painted, and black cloth surfaces. The copper signal was weaker and the aluminum noisier than from the steel surface. At higher laser powers, ablation of the painted surface occurred and resulted in an additional background signal. A range of power levels is capable of evaporating the absorbate for detection without disrupting the surface. No signal was seen for paraterphenyl coated onto anodized aluminum (undetermined thickness), clear plastic, tan cardboard, white ceramic, or teflon.

Effects of varying other parameters were checked under similar conditions. Signal levels did not seem to change much when the detection laser delay was varied between 10 and 240 μs. A few runs were also performed using 532-nm light from frequency doubling the evaporation Nd:YAG laser, at energy densities of approximately 0.2 J/cm^2. Good signal levels were seen for aluminum, steel, and copper substrates. Mass spectrometric experiments in vacuum have indicated that 532-nm evaporation is more efficient than the 1.06-μm fundamental for vaporizing RDX [19].

Ambient explosive detection methods, and any role laser evaporation can play in sample preparation, require operation in air not a vacuum. The above experiments were conducted with low-vacuum pumping in about 0.03 torr residual air. Laser vaporization of 10 monolayers extending into a plume 1 cm above the surface would correspond to a local pressure of 0.1 torr at 300 K. It is important to know how the signal and laser evaporation process might change at higher pressures of added air, closer to the ambient values. In a series of runs with up to 30 torr air, the magnitude of the peak signal did not vary compared to low pressure. Similar signal levels were also seen in later runs at 75, 200, and 760 torr. At pressures of 30 torr and above, after the initial signal died out (about 30 s or less), a new signal appeared, grew in intensity, and then declined. This did not depend on the continued irradiation by the IR laser, and may be attributable to UV photochemistry between the evaporated dye and oxygen to form new fluorescing molecules. At atmospheric pressure the transition between signal types was not resolvable in time. These experiments did not have rapid pumping to remove material between laser shots.

4 Discussion and conclusions

These initial experiments suggest that pulsed near-IR laser powers of 0.2 J/cm^2 are sufficient to quantitatively vaporize non-volatile organic molecules into the gas phase for analysis by LIF or MS techniques. The method appears to work in air as well as vacuum. Although some dependence on molecular size/vapor pressure may occur, the laser powers needed appear to be below molecular decomposition or substrate damage/ablation thresholds. However, not all surfaces are effective for laser evaporation at 1.06 μm; while metallic and opaque black absorbers were observed to be similarly efficient, white or transparent substrates and anodized aluminum failed to generate any signal from evaporation. While there is evidence in the time dependence of the signal that repeated heatings spread and exhaust the evaporation region, the initial heating appears to remove a substantial fraction of irradiated material and responds linearly to the deposited concentration. We can speculate that some melting occurs at the edge of the heated area, with migration into the depleted area and evaporation by a subsequent laser pulse, to explain the smaller signals at later times.

Pulsed laser evaporation from a metal surface occurs by efficient absorption in the near-surface layers from interaction of the intense oscillating electric field of the laser light with the metal's electrons, followed by energy transfer to lattice vibrations. More absorption and less reflection occur than in the normal low power situation. Theory of this process is well developed [7, 9–11], and the observed behavior of metal surfaces is as expected—except for the anodized aluminum. This surface is a thin doped oxide layer electrochemically applied and dark in color, and it is surprising that its transparency and thickness are sufficient to prevent evaporation. At high laser powers, we can ablate this surface layer and produce an LIF signal of longer fluorescence lifetime that we attribute to AlO or AlO_2. The dark substrates, like the metals, are similarly well heated to evaporative temperatures, indicating efficient absorption in the near IR in the near-surface layers. Heat loss into the interior is slower than for conducting metals, so a longer heated duration, lower required peak temperature, and weaker absorption to greater depth may apply. The mechanism will be different from that of the conducting metals, with a more conventional absorption process. Insufficient heating by absorption at 1.06 μm is apparent for the non-black, non-metallic materials. Other experiments using silica surfaces show ineffective 1.06-μm heating but successful vaporization of RDX at 10.6 μm with a pulsed CO_2 laser [10]. Direct heating of various nitro-explosives on silica with a 248-nm excimer laser has also been demonstrated [17]. So, other wavelengths may work for a wider range of surface materials.

Some questions do remain for further investigation, in preparation for application of laser vaporization to remote detection of explosive trace residues. Of particular concern is the inefficacy of certain surfaces, suggesting one possibility to explore—that operation at longer IR (or UV) wavelengths where most materials absorb will remedy this substrate selectivity. Spot size and laser pulse length are among the remaining variables to investigate. We would

also like to estimate the surface temperatures needed for evaporation, because avoiding molecular decomposition is also a consideration. Certain microscopic details also merit examination—the roughness of the surfaces is unknown and uncontrolled, the evenness or localized crystallization of the organic dye (or explosive) is uncertain and may vary, and the effects of large amounts of additional surface contaminants must be explored. Thick deposits of a variety of materials may more likely represent real environments. At some point when heating of the entire surface coverage reaches a notable fraction of the deposited laser power, insufficient energy will be available to volatilize all the material and sensitivity will drop. The NIST Chemistry WebBook [20] gives $E = 28$ kcal/mole as the heat of sublimation for paraterphenyl (estimated room temperature vapor pressure 10^{-5} torr), and adopting this value for dye evaporation energy requirements produces a requirement of 6×10^{-5} J/monolayer/cm^2. Vaporizing 33 monolayers would then use 1% of the applied laser power (at 0.2 J/cm^2). Continuing this example and assuming an evaporation A factor of 10^{14}/s and an 8-ns hot time from the laser pulse width (t), a temperature of $T = 1020$ K would be needed to produce 50% evaporation per laser pulse. Equation (13) of [7] gives an approximate determination of this fraction f:

$$-\ln(1-f) = At\mathrm{e}^{-1.02E/RT}, \tag{1}$$

where E is the sublimation energy. Thermal desorption studies of modest-size straight-chain alkanes from various crystal surfaces suggest much higher A factors [21, 22]. A pre-exponential factor of 10^{16}/s would imply a peak temperature of only 765 K to vaporize half of the paraterphenyl. A lower volatility compound would require higher power and temperature. Since bond scission enthalpies significantly exceed those for evaporation, little complication is expected from decomposition even over longer reaction times. For example, a C–C bond scission of 90 kcal/mole (and similar A factor) has only a 10^{-3} probability in 10 μs at 1000 K.

The simple theoretical model of pulsed laser heating for metal substrates [7] provides a simple formula (7) for an effective temperature rise from a triangular pulse:

$$\Delta T = (4/3)(P/K)(\kappa t/\pi)^{1/2}, \tag{2}$$

where P is the laser power (0.2 J/cm^2/$t = 8$ ns), K is the thermal conductivity of the substrate (0.8 W/cm/K for iron at 300 K), and κ is the thermal diffusivity (0.2 cm^2/s at 300 K). The computed peak surface temperature for these conditions is 1240 K, slightly above the kinetic requirement computed in the previous paragraph. Considering the various approximations and assumptions, this is good agreement and validation of the physical process model for the experiments.

One may also consider other analytical applications for such a better-characterized laser desorption process, involving various non-volatile surface adsorbates. Examples include soil contaminated by herbicides and pesticides (dinitro-o-cresol and parathion contain detectable NO_2 groups (like explosives)) and soot or atmospheric aerosols coated with carcinogenic fluorescing polynuclear aromatic hydrocarbons (PAHs).

Acknowledgements This work was supported by SRI IR&D funds. B. Krancevic was supported by an NSF Research Experiences for Undergraduates program at SRI, grant PHY-0649315. Thanks are due to Steve Young for taking the SEM images.

References

1. G.M. Boudreaux, T.S. Millere, A.J. Kunefke, J.P. Singh, P. Jagdish, F.-Y. Yueh, D.L. Monts, Appl. Opt. **38**, 1411 (1999)
2. J. Shu, I. Bar, S. Rosenwaks, Appl. Opt. **38**, 4705 (1999)
3. T. Arusi-Parpar, D. Helfinger, R. Lavi, Appl. Opt. **40**, 6677 (2001)
4. J.M. Rosen, C. Dickinson, J. Chem. Eng. Data **14**, 120 (1969)
5. S. Grossman, Proc. SPIE **2794**, 717 (2005)
6. D. Burgess Jr., R. Viswanathan, I. Hussla, P.C. Stair, E. Weitz, J. Chem. Phys. **79**, 5200 (1983)
7. D. Burgess Jr., P.C. Stair, E. Weitz, J. Vac. Sci. Technol. A **4**, 1362 (1986)
8. M. Handschuh, S. Nettesheim, R. Zenobi, J. Chem. Phys. **108**, 6548 (1998)
9. J.F. Ready, J. Appl. Phys. **36**, 462 (1965)
10. J.S. Morgan, W.A. Bryden, J.A. Miragliotta, L.C. Aamodt, Johns Hopkins APL Tech. Dig. **20**, 389 (1999)
11. X. Gu, H.M. Urbassek, Appl. Surf. Sci. **253**, 4142 (2007)
12. C. Mihesan, M. Ziskind, E. Therssen, P. Desgroux, C. Focsa, Chem. Phys. Lett. **423**, 407 (2006)
13. L. Robson, A.D. Tasker, K.W.D. Ledingham, P. McKenna, T. McCanny, C. Kosmidis, P. Tzallas, D.A. Jaroszynski, D.R. Jones, Int. J. Mass Spectrom. **220**, 69 (2002)
14. S. Alimpiev, S. Nikiforov, V. Karavanskii, T. Minton, J. Sunner, J. Chem. Phys. **115**, 1891 (2001)
15. S.D. Huang, L. Kolaitis, D.M. Lubman, Appl. Spectrosc. **41**, 1371 (1987)
16. C. Bauer, P. Geiser, J. Burgmeier, G. Holl, W. Schade, Appl. Phys. B **85**, 251 (2006)
17. J. Cabalo, R. Sausa, Appl. Opt. **44**, 1084 (2005)
18. A.D. Tasker, L. Robson, K.W.D. Ledingham, T. McCanny, P. McKenna, C. Kosmidis, D.A. Jaroszynski, Int. J. Mass Spectrom. **225**, 53 (2003)
19. J.D. White, H. Oser, Int. J. Mass Spectrom. (2008, to be published)
20. W.G. Mallard (ed.), *NIST Chemistry WebBook* (NIST-SRD 69) (NIST, 2005)
21. S.L. Tait, Z. Dohnalek, C.T. Campbell, B.D. Kay, J. Chem. Phys. **128**, 234308 (2006)
22. K.A. Fichthorn, K.E. Becker, R.A. Miron, Catal. Today **123**, 71 (2007)